JOURNAL OF Materials CHEMISTRY

Photocatalytic properties of $Ba_3Li_2Ti_8O_{20}$ sol–gel

A. Hernandez,[a] L. M. Torres-Martinez,*[a] E. Sanchez-Mora,[a] T. Lopez[b] and F. Tzompantzi[b]

[a]*Facultad de Ciencias Quimicas, Division de Estudios Superiores, Universidad Autonoma de Nuevo Leon, A. P. 1625, Monterrey, Nuevo Leon, Mexico. E-mail: ltorres@ccr.dsi.uanl.mx; Fax: (52) (8) 3 74 07 09*

[b]*Universidad Autonoma Metropolitana-Iztapalapa, Department of Chemistry, A. P. 55-534, 09340 México D.F., Mexico*

Received 18th October 2001, Accepted 24th June 2002
First published as an Advance Article on the web 24th July 2002

Samples of $Ba_3Li_2Ti_8O_{20}$ were prepared by the sol–gel method at pH 3 and 9 using acetic acid and ammonia hydroxide respectively as hydrolysis catalysts. The band gap (E_g) of the solids prepared was calculated from the UV-Vis absorption spectra of samples thermally treated at different temperatures, the values obtained ranging from 3.37 to 3.09 eV. The E_g values of the powders synthesized at pH 9 were higher than those of samples prepared at pH 3. Surface characterization of the solids was carried out from adsorption isotherms and FTIR studies, and their photocatalytic activities on 2,4-dinitroaniline degradation were also measured. The decomposition rate followed Langmuir–Hinshelwood kinetics. According to the calculated kinetic parameters, better results were obtained once the crystalline structure of $Ba_3Li_2Ti_8O_{20}$ had formed.

Introduction

Of the advanced oxidation processes, the process that uses heterogeneous reactions with photoreactive semiconductor powders has received much attention because of its application in the degradation of toxic organic compounds in water.[1] Hence, the development of new semiconducting materials with photocatalytic properties is very important. Of the semiconductor oxides usually used in heterogeneous photocatalysis, TiO_2, in both its anatase and rutile allotropic forms, has been the most widely studied.[2] In recent years, it has been widely demonstrated that the interaction between ultraviolet radiation and titanium dioxide has a big potential for the destruction of toxic organics in industrial wastewater.[3]

Various catalysts have been used for this purpose, such as CdS[4] and α-Fe_2O_3.[5] SnO_2 has also been probed as a photocatalyst because of its properties which are similar to those of TiO_2, except it has a higher band gap energy (3.5 eV).[6]

Titanium oxide has chemical and electrical properties that make it an attractive material for different applications. When this compound is pure and stoichiometric it shows dielectric properties, however, if the elemental ratio Ti : O (1 : 2) is changed, it shows semiconductor properties. Semiconductive titania can be used in photoelectric devices, photovoltaic cells, electrochromic electrodes, *etc.*[7,8] The semiconductor properties of titanium oxide basically depend on point defect density in the crystalline structure and impurity concentration in the sample.[9,10]

Measurement of the band gap energy is a discriminating method for the *in situ* study of semiconducting properties. Thus the determination of the band gap by UV-Vis spectroscopy is an alternative method for the study of stoichiometry deficiency and this gives us an idea of the number of defects in the material.[11,12]

When a semiconductor powder is illuminated with photons of sufficient energy (band gap energy, E_g, or greater) a photon ($h\nu$) excites an electron from the valence band to the conduction band and leaves an electronic vacancy (h_{vb}^+) in the valence band.[13] Two possible oxidation processes can occur during the photocatalytic reactions: water can be oxidized to hydroxyl radicals by photogenerated positive holes and then these react with organic substrates to produce oxidized species:

$$\text{Catalyst} + h\nu \rightarrow e^- + h^+ \quad (1)$$

$$e^- + O_2 \rightarrow O_2^- \quad (2)$$

$$h^+ + H_2O \rightarrow {}^{\bullet}OH + H^+ \quad (3)$$

or organic solute compounds can be oxidized directly at the surface of the catalyst by photoproduced holes during the interaction with UV light.

$$\text{Catalyst} + h\nu \rightarrow e^- + h^+ \ (h\nu \geqslant E_g) \quad (4)$$

$$O^-_{x(\text{ads})} + h^+ \rightarrow x/2\ O_2(g) \text{ with } x = 1 \text{ or } 2 \quad (5)$$

The generation rate of electrons and holes is proportional to the photon flux. Subsequently the photodesorption of negatively charged adsorbed species (*i.e.* oxygen species) occurs by reaction with h^+. The accumulated electrons favor recombination:

$$e^- + h^+ \rightarrow N + \text{Energy (N = neutral center)} \quad (6)$$

An alternative way to increase the efficiency of the photocatalytic processes and to reduce the required energy of the radiation is to develop more active catalysts.

In photocatalysis the catalytic activity of a semiconductor is not only determined by the electronic properties, but also by particle size, surface area and its crystallinity. The chemical history of the sample is also very important.[14–19] Recent studies of photocatalytic processes have focused on the surface and/or bulk modification of the semiconductor. The structure of the final semiconductor powder depends on the synthesis method. The sol–gel process allows the preparation of materials with specific features which are determined by several parameters, such as reaction pH, stability of the reactants, the amount of water, refluxing temperature and alkoxide nature. A few papers have been published about sol–gel material photocatalysts.[20]

Recently we reported the synthesis of the semiconductor

 DOI: 10.1039/b109593p

compound $Ba_3Li_2Ti_8O_{20}$, whose composition is 8.3% Li_2O, 25%BaO and 66.7% TiO_2,[21] by means of the sol–gel process under acidic and basic conditions.[22] In this publication we present the study of the photocatalytic activity of this ternary oxide whose tunnel structure is associated with its catalytic behaviour in heterogeneous reactions.[23] The values of the band gap were calculated from UV-Vis absorption spectra of the semiconductor powders; the surface adsorbed water, hydroxy groups and surface area were also analyzed. The purpose of this study was to investigate the influence of the synthesis conditions of $Ba_3Li_2Ti_8O_{20}$ on the photocatalytic degradation of 2,4-dinitroaniline in aqueous solution. The decomposition of many organic pollutants by photocatalytic processes follows Langmuir–Hinshelwood kinetics.[20,24] Therefore in this work the decomposition rates were determined and the kinetic parameters were calculated from the experimental rate data.

Experimental

Sample preparation

Barium isopropoxide (Aldrich Chemicals, 99.9%), lithium acetate dihydrate (Sigma, 63.4%) and titanium isopropoxide (Aldrich Chemicals, 97%) were the metallic precursors. Ethanol (99.9% PROQUIM) was used as solvent and glacial acetic acid (PROQUIM 99.8%) was added under continuous stirring to give pH 3. The reaction mixture was refluxed at 70 °C. In order to prepare the same compound under different pH conditions, ammonia hydroxide was used instead of acetic acid. Opaque gels were obtained which were dried in the oven at 90 °C for 24 hours (fresh sample). Different portions were fired in an electrical furnace at 400, 600 and 800 °C for 6 hours.

Characterisation

UV-Vis spectroscopy. The UV-Vis absorption spectra of the samples were obtained by diffuse reflectance studies using a Perkin Elmer spectrophotometer model Lambda 12 coupled to an integration Labsphere RSA-PE-20. A Spectralon standard USRS-99010 with 100% reflectance was used as reference.

Specific surface area and pore size distribution analysis. Nitrogen adsorption isotherms of the samples were measured by a gas sorption instrument (Micromeritics ASAP 2000). The surface area was calculated by the BET equation. The BJH method was used to calculate the mean pore size diameter distribution. All samples were degassed at 200 °C for 6 h before analysis.

X-Ray diffraction technique. The samples were analyzed by a Siemens D-5000 diffractometer with Cu-Kα radiation (λ = 1.5418 Å).

FTIR spectroscopy. The hydroxy groups on the catalysts were studied by infrared absorption spectroscopy using a Perkin Elmer FT-IR Spectrometer Paragon 1000 PC. The samples were mixed with KBr and pressed under 7 tons cm^{-2} to obtain a transparent pellet.

Photocatalytic activity

Photocatalytic experiments were carried out at room temperature. A quantity of 200 mg of each catalyst was added to a flask containing 500 ml of an aqueous solution of 2,4-dinitroaniline at 30 ppm. Under stirring, the solution was irradiated in a closed box with a UV lamp Black-Ray model XX-15, which emits radiation at λ = 254 nm and an intensity of 1600 μW cm^{-2}. The light intensity received by the vessel was 1560 μW cm^{-2}, measured with a UVP radiometer model UVX-25 with a 254 nm sensor. The reaction rate was followed by taking aliquots every 10 min which were then analyzed in a UV-Vis Hewlett-Packard model 8452 spectrophotometer equipped with a diode array as detector. The concentration of 2,4-dinitroaniline was calculated from the absorption band at 346 nm.

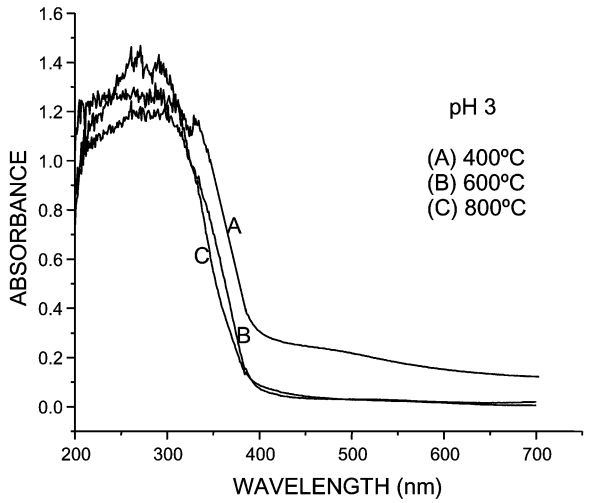

Fig. 1 UV-Vis spectra of barium lithium titanate sol–gel catalyst synthesized at pH 3 and heated at different temperatures.

Results and discussion

Band gap energy

The UV-Vis spectra (diffuse reflectance) of the samples prepared at pH 3 are shown in Fig. 1. The UV-Vis spectra of the samples prepared at pH 9 were similar to those of the materials obtained at acidic pH, showing a displacement of the absorption edge towards higher energy values.

In this work the values of the band gap energy of the samples annealed at different temperatures were calculated by using the equation $\alpha(h\nu) = A(h\nu - E_g)^{m/2}$, where α is the absorption coefficient, $h\nu$ is the photon energy, A is a constant and $m = 1$ represents a direct transition between bands (valence band and conduction band). E_g was calculated from the UV-Vis spectra by extrapolating a straight line from the absorption curve to the abscissa axis. When α is zero, then $E_g = h\nu$.[25]

The E_g values calculated for each sample are reported in Table 1. When the samples are synthesized at pH 9 using NH_4OH as the hydrolysis catalyst in the gelation reaction, the E_g values are higher than those of the samples prepared at pH 3. The hydrolysis reaction is much faster in acid media than polycondensation and the gel obtained is highly hydroxylated.[26] With an increase in solution pH, the condensation reaction predominates, hence, the gels obtained have less OH groups and so tend to have a small amount of structural defects. When the gel is prepared at pH 9, it is less hydroxylated and the formation of defects by dehydroxylation is small.[12] This was confirmed by the FTIR spectra of the samples annealed at 800 °C where the sample prepared at pH 3 shows a stretching band at 3440 cm^{-1} typical of hydroxy groups, whereas in the spectra of the sample at pH 9, this band is very small.[22]

Table 1 Band gap values for lithium barium titanate samples

	E_g/eV		
Synthesis pH	T = 400 °C	T = 600 °C	T = 800 °C
3	3.09	3.14	3.18
9	3.48	3.44	3.37

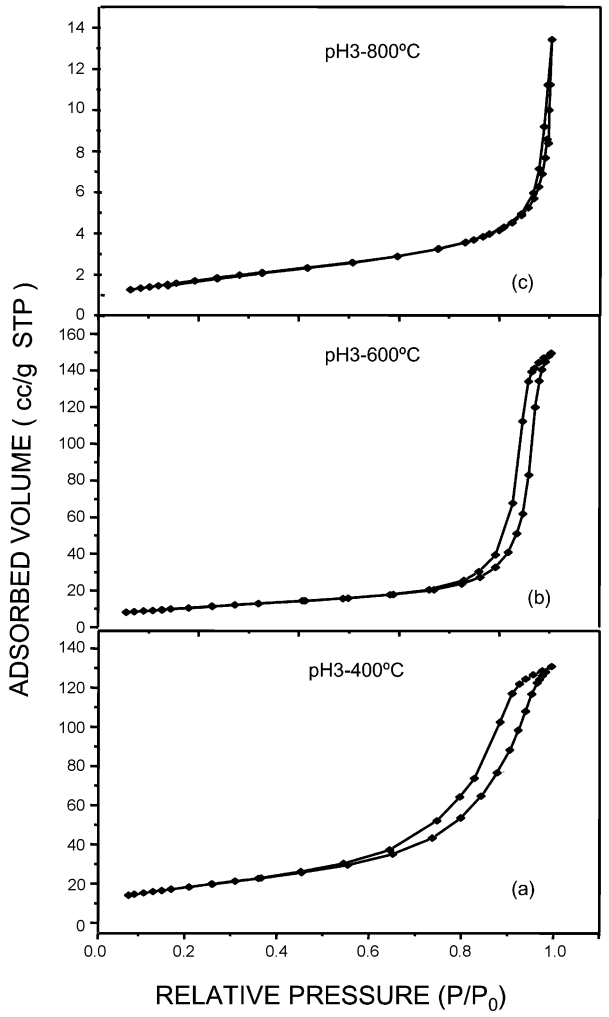

Fig. 2 Nitrogen adsorption isotherms for the barium lithium titanate sol–gel catalyst synthesized at pH 3 and heated at different temperatures.

The samples synthesized at pH 3 have similar band gap values as the temperature is increased. These values are close to those reported for TiO_2 (3.1–3.2 eV).[13] In the samples prepared at pH 9 the E_g values decrease as the temperature is increased and tend to the E_g value of rutile TiO_2 due to the elimination of the OH groups that are bonded to the material.

Textural properties

Fig. 2 shows the nitrogen adsorption isotherms for the samples synthesized at pH 3. The isotherm illustrated in Fig. 2a is a type IV isotherm which is characteristic of a porous adsorbent with pore radius in the range of mesopores (20–500 Å). This type of hysteresis is correlated with the pore shape. In this case the hysteresis observed corresponds to type B, according to Boer's classification,[27] and is associated with slit-shaped pores. In the samples annealed at higher temperatures (Figs. 2b and c) the isotherms are similar to type III, characterized by a small adsorbate–adsorbent interaction. The lack of hysteresis in desorption, with increasing temperature, is due to the diminution of the porosity.[28]

The isotherms obtained from the samples synthesized at pH 9 (not shown) correspond to type V, also being a result of a small adsorbate–adsorbent interaction similar to those of type III. The loop of hysteresis is small, which shows a low porosity in these materials.[29]

Table 2 shows data of specific surface areas and average pore diameters for samples calcined from 400 to 800 °C. BET areas gradually decrease as the temperature is increased, whereas the pore size increases on heating from 400 to 600 °C due to desorption of substances physisorbed in the gel during the drying process. However, in the samples annealed at 800 °C the pore size diminishes due to network contraction, which is confirmed by the measured average pore diameter. When the samples were synthesized at basic pH, the specific surface areas were greater than those synthesized under acidic conditions. The sample obtained at pH 9 and annealed at 400 °C shows a high specific surface area of 117 $m^2\ g^{-1}$.

Table 2 Specific surface area and average pore size of sol–gel samples obtained at different pH

Temperature/ °C	pH	BET surface area/$m^2\ g^{-1}$	Pore diameter/Å
400	3	66.51	121.55
600	3	38.08	240.15
800	3	6.17	93.98
400	9	117.83	109.03
600	9	49.30	—
800	9	9.37	76.75

Comparing the values of the average pore size of the samples prepared at different pH, it appears that the synthesis at acidic pH facilitates the formation of bigger pores. However, analysis of the mean pore size diameter distribution, by means of the BJH method, indicates that the samples synthesized under basic conditions show bimodal distributions, one of which tends towards the range of macropores (1000–2000 Å), whereas in the samples prepared at acidic pH, the distribution remains in the range of the mesopores showing a monomodal distribution. This behaviour is attributed to the fact that acidic hydrolysis of the sol–gel facilitates the formation of small pores and basic conditions facilitate the formation of bigger pores.[30]

Photocatalytic activity

The catalytic activity of the samples was studied using, as a test reaction, the decomposition of the 2,4-dinitroaniline at room temperature. This toxic organic substance is used in the textile industry and it is harmful to the aquatic environment.[31]

The UV-Vis spectra of the 2,4 dinitroaniline at different reaction times was registered in the 600–200 nm wavelength range. The spectra showed two main absorption bands at 346 nm and 262 nm. Such bands diminish gradually until they disappear, which indicates that the organic compound photodecomposition is complete. The decomposition of the substrate was followed by monitoring the UV absorption band at 346 nm. The decomposition of the substrate as a function of time with the catalyst prepared at pH 3 is shown in Fig. 3. A similar graph was obtained for the catalyst prepared at pH 9.

For the correct evaluation of data we applied the Langmuir–Hinshelwood model using the equation for heterogeneous photocatalytic reactions in a batch reactor:[32]

$$-V\frac{dC}{dt} = \frac{mAk_1C}{1+k_2C}$$

where V is the liquid volume, C the substrate concentration, t the time, m the mass of catalyst, A the adsorption sites per g of catalyst, k_1 the apparent rate constant and k_2 the apparent adsorption constant.

Integrating from $t = 0$ to $t =$ i and for the initial concentration C_0 to the C_i concentration at $t =$ i, we have:

$$\frac{\ln\frac{C_0}{C}}{C_0-C} = -k_2 + \frac{mAk_1k_2t}{V(C_0-C)}$$

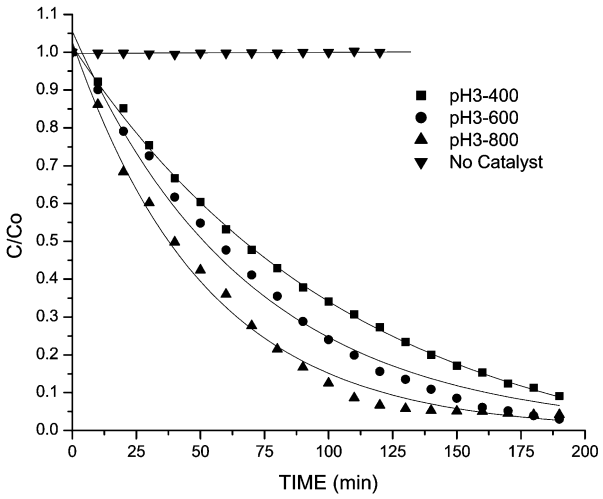

Fig. 3 Photodecomposition as a function of time of the 2,4-dinitroaniline on the barium lithium titanate sol–gel catalyst synthesized at pH 3 and annealed at different temperatures.

And finally, to estimate the time in which $C = C_0/2$, we use:

$$t_{1/2} = \frac{\left(\frac{0.693}{k_1 k_2} + \frac{C_0}{2k_1}\right)}{\frac{mA}{V}}$$

The values of k_1, k_2, k_1k_2 (apparent reactivity) and $t_{½}$ (apparent half-life) for the catalysts obtained at different temperatures in the decomposition of 2,4-dinitroaniline are tabulated in Table 3. These data were estimated from a graph of $(\ln (C_0/C))/(C_0 - C)$ against $t/(C_0 - C)$.

The activity expressed as $t_{½}$ for the catalysts prepared at pH 3 shows that degradation is favoured by the sample annealed at 800 °C ($t_{½} = 26$ min). According to high k_2 value we can see that the adsorption capacity of this catalyst is favoured due to its higher degree hydroxylation, hence the OH groups behave as adsorption centres. At this temperature (800 °C), the crystalline structure of $Ba_3Li_2Ti_8O_{20}$ is formed according to XRD studies.[21,22] For the catalyst synthesized at pH 9 the photodegradation is improved with the samples fired at 600 and 800 °C. Under basic conditions the sample calcined at 800°C has the same crystalline structure as that calcined under acidic con- ditions, however, it has lost almost all its hydroxy groups causing a high degree of defects yielding vacancies (V). In this sample the formation of defects can occur by two different mechanisms: one of them is due to a dehydroxylation process:

$$2OH^- \rightarrow H_2O + V_{O^{2-}}{}^{+} + e^- + O^{2-}$$

and the other one is due to desorption of surface oxygen; the formation of an oxygen vacancy is given by the Kroger–Vink notation:[32]

$$O_O \leftrightarrow V_O + 2_{cb}{}^{e^-} + ½O_2$$

Defects in an oxide semiconductor are linked to electronic properties. According to the calculated k_1 value, in this sample, electronic transference is favoured and it shows a good activity towards 2,4-dinitroaniline decomposition. However, the adsorption capacity is low due to material sintering that takes place onthermal treatment. Moreover, combination of the apparent rate constant (k_1) and the apparent adsorption constant (k_2) gives a similar apparent reactivity (0.066 and 0.062) for the compound $Ba_3Li_2Ti_8O_{20}$ obtained at 800 °C for both synthesis conditions.

Table 3 Results of the Langmuir–Hinshelwood model for 2,4-dinitroaniline decomposition on sol–gel catalysts

pH	Temperature/ °C	k_1/ 10^6 min^{-1}	k_2/ M^{-1}	k_1k_2/ min^{-1} M^{-1}	$t_{½}$/ min
3	400	9.4	4115	0.039	44
3	600	43.4	1220	0.053	33
3	800	7.1	9300	0.066	26
9	400	15.2	2117	0.032	54
9	600	40.7	1762	0.072	24
9	800	35.4	1744	0.062	28

It is noticeable that in the sample prepared at pH 9 and heated at 600 °C, the activity expressed as $t_{½}$ is closer to those calculated for the samples annealed at 800 °C. Previous work on the TiO_2 sol–gel synthesis[33] showed that at pH 3 and 9 the anatase form is present with small percentages of the rutile form when the samples are annealed at lower temperatures (200–600 °C). At temperatures above 600 °C the acidic pH stabilized the rutile form, whereas at pH 9 the anatase form is stabilized. In this work, as the temperature is increased, the structure of the solid formed changes from anatase to barium titanate and finally to $Ba_3Li_2Ti_8O_{20}$.[21] Previous work on photodegradation of different organic compounds in water showed that the anatase form is more active than the rutile phase.[34] At 600 °C (pH 9) $Ba_3Li_2Ti_8O_{20}$ is amorphous and therefore is not detectable with the XRD Siemens D5000 equipment.[22] At this temperature the phase is dispersed on titania (especially anatase) and the catalytic activity is improved. Specialized studies in this area are in progress using the Rietveld method.

Conclusions

From these results we can conclude that the synthesis conditions influence the properties of the catalysts. The E_g values depend on both pH and thermal treatment synthesis parameters. The specific surface area did not influence the catalytic activity. However, dehydroxylation of the thermally treated samples had an important effect on the photocatalytic properties. The best degradation rate is shown by the catalyst obtained at 800 °C when the crystalline phase $Ba_3Li_2Ti_8O_{20}$ is already formed. Therefore, it seems that the crystal structure is an important factor which has to be considered in the photocatalytic process.

Acknowledgements

Financial support from the CONACyT (Grants 35415-U and 33467-E) and the Universidad Autonoma de Nuevo Leon (PAICYT CA549-01 and CA379-00) is gratefully acknowledged. A. Hernandez wishes to thank the CONACyT for the award of the scholarship No. 92583.

References

1 Y. Nosaka, M. Kishimoto and J. Nishino, *J.Phys. Chem. B*, 1998, **102**, 10279.
2 A. Sclafani and J. M. Herrmannn, *J.Phys. Chem.*, 1996, **100**, 13655.
3 S. Malato, C. Richter, J. Galvez and M. Vincent, *Sol. Energy*, 1996, **56**, 401.
4 W. Z. Tang and C. P. Huang, *Water Res.*, 1995, **24**, 543.
5 S. Espuglas, P. L. Yue and M. I. Pervez, *Water Res.*, 1994, **28**, 1323.
6 A. Nanthakumar and N. R. Armstrong, *Semiconductor Electrodes*, ed. H. O. Finklea,Elsevier, New York, 1988.
7 B. Aurian-Blajeni, M. Hamann and J. Manasen, *J. Sol. Energy*, 1980, **25**, 165.
8 K. Hirano and A. J. Bard, *J. Electrochem. Soc.*, 1980, **127**, 1056.
9 R. D. Shanon, *J. Appl. Phys.*, 1964, **35**, 3414.
10 Y. Xu, Z. Zhu, W. Chen and G. Ma Chin, *J. Appl. Chem.*, 1991, **8**, 28.
11 M. Ampo, T. Shima, S. Kodama and Y. Kubokawa, *J. Phys. Chem.*, 1987, **91**, 4305.

12 E. Sánchez and T. López, *Mater. Lett.*, 1995, **25**, 271.
13 P. Rominder and S. Suri, *Water Environ. Res.*, 1993, **65**, 665.
14 C. K. Chan, J. F. Porter, Y. G. Li, W. Guo and C.-M. Chan, *J. Am. Ceram. Soc.*, 1999, **82**, 566.
15 A. Sclafani, L. Palmisano and M. Schiavello, *J. Phys. Chem.*, 1990, **94**, 829.
16 Y. Ku and C. Hsieh, *Water Res.*, 1992, **26**(11), 1451.
17 J. Chen, D. F. Ollis, W. H. Rulkens and H. Bruning, *Water Res.*, 1999, **33**(3), 661.
18 J. Chen, D. F. Ollis, W. H. Rulkens and H. Bruning, *Water Res.*, 1999, **33**(3), 669.
19 C. J. Brinker, R. Sehgal, N. K. Raman, S. S. Prakash and L. Delattre, *Mater. Res. Soc. Symp. Proc.*, 1995, **368**, 329.
20 T. Lopez, J. Hernandez-Ventura, R. Gomez, F. Tzompantzi, E. Sánchez, X. Bokhimi and A. Garcia, *J. Mol. Catal.*, 2000, **2995**, 1–7.
21 A. Hernandez, L. M. Torres-Martinez and T. López, *Mater. Lett.*, 2000, **45**, 340.
22 A. Hernandez, L. M. Torres-Martínez and T. Lopez, *Mater. Lett.*, 2002, **45**, 62.
23 Y. Inoue, T. Kubokawa and K. Sato, *J. Phys. Chem.*, 1991, **95**, 4059.
24 T. Lopez, R. Gomez, E. Sanchez, F. Tzompantzi and L. Vera, *J. Sol-gel Sci. Tech.*, 2001, **22**, 99.
25 L. A. Grumes, R. D. Leapman, C. N. Wilker, R. Hoffmann and A. B. Kuns, *Phys. Rev. B: Condens. Matter*, 1982, **25**, 7157.
26 T. López, E. Sánchez, P. Bosch, Y. Meas and R. Gomez, *Mater. Chem. Phys.*, 1992, **32**, 141.
27 S. Lowell and J. E. Shields, *Powder Surface Area and Porosity*, Chapman & Hall, New York, 3rd edn., 1991.
28 C. J. Brinker and G. W. Scherer, *Sol-gel Science*, Academic Press, London, 1990.
29 S. J. Gregg and K. S. W. Sing, *Adsorption surface area and porosity*, Academic Press, 1982.
30 R. D. Gonzalez, T. Lopez and R. Gomez, *Cat. Today*, 1997, **35**, 293.
31 KEMI 2/97, Kemikalieinspektionen, Solna, Sweden. February 1997, Swedish.
32 E. Pelizzetti and N. Serpone, *Photocatalysis, Fundamentals and Applications*, Wiley Interscience, 1989.
33 A. Bokhimi, O. Morales, T. Novaro, E. Sánchez Lopez and R. Gomez, *J. Mater. Res.*, 1995, **10**(11), 2788.
34 Z. Ding, G. Q. Lu and P. F. Greenfield, *J.Phys. Chem. B.*, 2000, **104**, 4815.